Available online at www.sciencedirect.com
SCIENCE DIRECT®
Chemical Physics Letters 378 (2003) 1–8
CHEMICAL PHYSICS LETTERS
www.elsevier.com/locate/cplett

Deoxyadenosine sugar puckering pathway simulated by the stochastic difference equation algorithm

Karunesh Arora, Tamar Schlick *

Department of Chemistry and Courant Institute of Mathematical Sciences, 251 Mercer Street, New York University, New York, NY 10012, USA

Received 3 June 2003; in final form 11 July 2003
Published online: 8 August 2003

Abstract

The conformational transition pathway of sugar puckering between the C2′-endo and C3′-endo conformations of deoxyadenosine (dA) is reported using the stochastic difference equation (SDE) algorithm, which approximates long-time pathways. The south pucker is favored over the north by 0.34 ± 0.2 kcal/mol, and the free energy barrier is about 2.2 ± 0.2 kcal/mol above the global minimum. The transition occurs through the east barrier, with significant decrease in puckering amplitude near the barrier. These results are consistent with prior studies on sugars in nucleic acids and indicate that the SDE has potential for large nucleic acid and nucleic acid/protein systems.

1. Introduction

Molecular dynamics (MD) and Brownian dynamics (BD) simulations have become important resources for revealing detailed insights into the structure and function of complex systems on range of spatial scales [1,2]. Recent coupled quantum mechanical/molecular mechanical (QM/MM) simulations also offer impressive details of chemical reactions [3]. Since standard MD simulations are still limited to timescales of a few nanoseconds, there has been growing interest in developing novel methods that capture large-scale conformational rearrangements, such as subdomain motions in DNA polymerases and chromatin condensation.

If the initial and final states are known, biomolecular systems can be treated with microscopic coupled QM/MM methods (e.g., EVB method [3]), or 'steered' or targeted (see [2], and references therein) – subjected to time-dependent external forces along certain degrees of freedom or along a local free-energy gradient – to study chemical reactions, probe molecular details of experiments, study folding/unfolding events, or generate insights into disallowable configurational states as well as conclusions regarding common pathways [4,5]. Targeted dynamics methods, however, employ large biasing potentials ($\gg k_B T$) to capture large-scale conformational transitions, and the

* Corresponding author. Fax: +1-212-995-4152.
E-mail address: schlick@nyu.edu (T. Schlick).

0009-2614/$ - see front matter © 2003 Elsevier B.V. All rights reserved.
doi:10.1016/S0009-2614(03)01195-3

resulting pathways cannot be related to known statistical ensembles at room temperature.

The stochastic difference equation (SDE) algorithm of Elber et al. [6] provides a numerically stable solution at arbitrary timesteps by a suitable path approximation. This advantage makes it possible to study dynamic processes at extended timescales. SDE is based on optimization of a classical action and is thus useful in the investigation of processes where reactant and product states are known. The SDE and its variants have been used to follow dynamics of biological processes on timescales varying from milliseconds to microseconds including, hemoglobin's R to T transition, C peptide's folding, ion permeation through a gramicidin ion channel, cyclodextrin glycosyltransferase's mechanism, protein A's folding pathways, and the kinetics of cytochrome C's folding (see citations in [7]). In this work, we develop and apply SDE for the first time to a nucleic acid system, namely the conformational transition pathway of sugar repuckering in a deoxyadenosine (dA) nucleoside.

It is now well established that the deoxyribose sugar plays an important role in the structure of nucleic acids. The overall conformation of a nucleoside can be described by the glycosyl torsion angle (χ), backbone torsion (γ), and phase angle of pseudorotation (p), which effectively defines the sugar conformation based on a wave-like motion from a chosen mean plane defined by five ring atoms (ν_0 to ν_4) (see Fig. 1 and Eq. (3)). Theoretically, the pseudorotation angle can vary between 0° and 360°, but is usually limited to the physiological subrange from −20° to 200°. The sugar pucker conformational space for standard DNA is characterized by two energy minima at C3′-endo and C2′-endo conformations, also called north and south ranges, centering around $p = 18°$ and $p = 162°$, respectively. These are characteristics of A-form and B-forms of DNA, respectively. The associated value of glycosyl torsion is A-DNA-like, or $\chi = 201.1°$ in C3′-endo, and B-DNA-like with $\chi = 258.1°$ in the C2′-endo conformation.

There have been many theoretical studies of sugars in nucleic acids. In the late 1970s, Levitt and Warshel pioneered, with Lifson and Warshel's newly developed Cartesian coordinate consistent force-field approach [8], a rigorous adiabatic mapping to investigate the variation of energy along the pseudorotation path. Their energy barrier of 0.6 kcal/mol between C2′-endo and C3′-endo deoxyribose conformations [9] implies frequent interconversion at room temperature, as

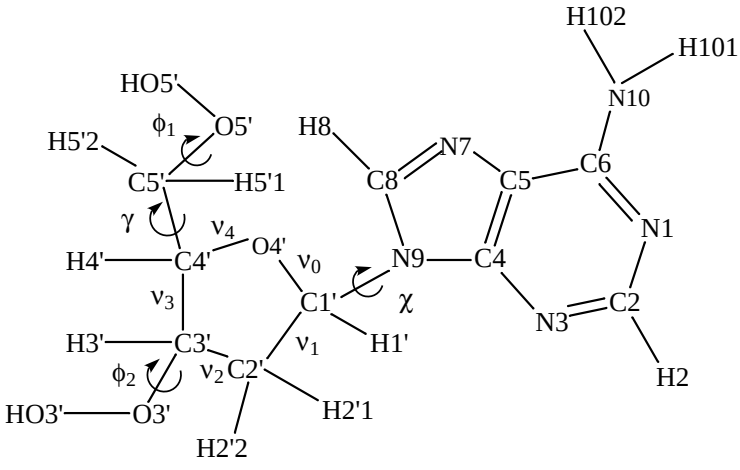

Fig. 1. Schematic representation of the deoxyadenosine nucleoside. The labeled torsional degrees of freedom are denoted as: γ, O5′–C5′–C4′–C3′; χ, O4′–C1′–N9–C4; ν_0, C4′–O4′–C1′–C2′; ν_1, O4′–C1′–C2′–C3′; ν_2, C1′–C2′–C3′–C4′; ν_3, C2′–C3′–C4′–O4′; and ν_4, C3′–C4′–O4′–C1′. The torsions ϕ_1, C4′–C5′–O5′–HO5′ and ϕ_2, C4′–C3′–O3′–HO3′ describe the rotation about the hydroxyl bonds; they do not affect the overall conformation of a nucleoside.

observed in dynamics simulations [10,11] and deviating from an assumption of high energy barrier [12]. Olson and Sussman's [13] statistical analysis estimated the barrier to be 2–5 kcal/mol. Olson's [14] later molecular mechanics calculation that did not allow full structure relaxation stressed the gauche effect as an important factor in reproducing the properties of deoxyribose in solution and refined the estimate to about 2 kcal/mol [14]. Indeed, subsequent studies produced lower values (1.5 kcal/mol, Harvey and Prabhakaran [10]). Methods that do not reflect the sugar in its ambient solvent environment produce other values, typically higher (>4 kcal/mol, Foloppe and MacKerell [15], by high-level ab initio quantum mechanical calculations; 3.2 kcal/mol, Schlick et al. [16], by energy minimization; and 1–2 kcal/mol, Nilsson and Karplus [17], also by energy minimization).

Our motivation for this work is an application of the SDE method to a large DNA polymerase complex (DNA bound to primer/template) system to study polymerase mechanisms [18]. Though the SDE algorithm is implemented in the MOIL software [19] and available to the public, a nucleic acid force field (AMBER) had to be incorporated and carefully tested. Results of our study of the dynamics and energetics of the sugar ring in nucleosides suggest that the C2′-endo conformation of deoxyadenosine is thermodynamically favored over the C3′-endo conformation. The transition occurs through an east pseudorotation energy barrier with a decrease in the amplitude of the furanose ring as it passes over the barrier. The free energy barrier for the transition is 2.2 ± 0.2 kcal/mol. Results are in agreement and further confirm the previous estimates on nucleosides [9,10,14,17,20]. Though, of course the barrier between the two minima of deoxyadenosine C2′-endo and C3′-endo states is not more than few kcal/mol, and thus even standard MD can be used to sample the sugar conformational space and generate an ensemble for reliable estimation of thermodynamic free energies, our current study on the free nucleoside serves as the benchmark for future work on applying SDE with the AMBER nucleic acid force field to protein/DNA systems.

2. Methods

2.1. The SDE method

The SDE algorithm developed by Elber et al. [21] is based on the formulation of molecular dynamics as a boundary value problem. For specified coordinates of initial (Y_1) and final conformation (Y_2), (mass-weighted) coordinates (Y) are solved as a function of the trajectory length l. A search is made for a trajectory that makes the action (S) stationary, where the action is expressed as

$$S = \int_{\vec{Y}_1}^{\vec{Y}_2} \sqrt{2(E-U)}\,\mathrm{d}l. \tag{1}$$

Here E is the total energy, U is the potential energy, and $\mathrm{d}l$ is a length element. The (fixed) endpoints $\vec{Y}_1$ and $\vec{Y}_2$ are coordinates of dA's C2′-endo and C3′-endo conformations, respectively. SDE uses a discretized version of the action $S \cong \sum_i \sqrt{2(E-U)}\Delta l_{i,i+1}$ to define the classical trajectory. According to *the principle of least action*, a stationary point of S exists (S need not be a minimum or maximum); a trajectory that makes S stationary also solves the classical equations of motion. Such a trajectory is computed by optimizing the gradient norm given by the following target function T_G:

$$T_G = \sum_i \left(\frac{\partial S/\partial Y_i}{\Delta l_{i,i+1}}\right)^2 \Delta l_{i,i+1} + \lambda \sum_i (\Delta l_{i,i+1} - \langle \Delta l \rangle)^2, \tag{2}$$

where the variables Y_i from 0 to $N+1$ are all the structures along the path, and the parameter λ defines the coupling strength of a restraint that maintains the structures equally distributed along the trajectory ($\langle \Delta l \rangle = 1/(N+1)\sum \Delta l_{i,i+1}$). For sufficiently small steps, $\Delta l_{i,i+1}$, the exact classical trajectory is recovered. T_G is minimized subject to additional constraints to keep the rigid body translations and rotations constant [22]. Two major assumptions in the application of the SDE method are the use of the implicit Born solvation model [23–25] and the filtering of high-frequency motions [21]. The former can be alleviated using greater computer time, but the filtering makes SDE applicable to long-time trajectories.

Note that the trajectories are parameterized as a function of length and not time according to recent formulations [21]. For a comparison of the formulations and their evaluation, see [6]. An overview of the SDE method and its computational efficiency are provided elsewhere [6,21].

2.2. Sugar conformation description

The sugar puckering pseudorotation angles (p) and puckering amplitude ($\nu_{\max}$) used to describe the conformational state of the sugar are determined following the work of Rao, Westhof, and Sundraligam (RWS) [26]. In the original work [27], Altona and Sundraligam (AS) calculate the furanose puckering phase angle p from the following formula:

$$p = \tan^{-1}\left[\frac{(\nu_4 + \nu_1) + (\nu_3 + \nu_0)}{2\nu_2(\sin 36^\circ + \sin 72^\circ)}\right]. \tag{3}$$

Here, the ν_i are the five endocyclic torsion angles: ν_0, C4′–O4′–C1′–C2′; ν_1, O4′–C1′–C2′–C3′; ν_2, C1′–C2′–C3′–C4′; ν_3, C2′–C3′–C4′–O4′; and ν_4, C3′–C4′–O4′–C1′. The sugar puckering amplitude ($\nu_{\max}$) measures the extent of deviations of torsion angles from zero and is described as follows:

$$\nu_{\max} = \nu_2/\cos p. \tag{4}$$

However, in the AS method, the value of $\nu_{\max}$ depends on the choice of origin atom (i.e., O4′ atom opposite ν_2). To overcome this shortcoming, Rao et al. (RWS) describe a better formulation based on an approximate Fourier analysis which treats all the endocyclic torsions equally [10,26], as follows:

$$A = \frac{2}{5}\sum_{j=0}^{4}\nu_j\left(\frac{4\pi j}{5}\right),$$

$$B = -\frac{2}{5}\sum_{j=0}^{4}\nu_j\left(\frac{4\pi j}{5}\right),$$

$$\nu_{\max}^2 = (A^2 + B^2), \tag{5}$$

$$p = \tan^{-1}\left(\frac{B}{A}\right). \tag{6}$$

From experimental structures, typical C3′-endo state lies in the N (north) range of pseudorotational values, $-1^\circ \leqslant p \leqslant 34^\circ$, and the C2′-endo is in the S (south) range, $137^\circ \leqslant p \leqslant 194^\circ$. Here, we use the term C3′-endo and C2′-endo to denote these ranges rather than a localized set of specifically puckered states.

2.3. Preparation of C2′-endo and C3′-endo states of deoxyadenosine

Since the stochastic difference equation algorithm is based on a boundary value formulation, the coordinates of the initial and final states must be specified. The published Cartesian coordinates for the deoxyadenosine in C2′-endo and C3′-endo energy minima computed at MP2/6-31G* level of theory were obtained [15]. Ten molecular dynamics simulations of 1 ns each at 300 K were performed starting from these structures corresponding to north and south energy minima. The molecular dynamics module in MOIL [19] was used to perform these computations. The force field in MOIL is AMBER parm99.dat parameter set [28]. The equations of motion were integrated using the Velocity Verlet Verlet algorithm with a timestep of 1 fs. All van der Waals and electrostatic cutoffs were considered (i.e., no cutoffs were applied), and the nonbonded list was updated every 10 steps. The dielectric constant was set to unity, and 1–4 scaling factors were set as 2 and 8 for electrostatic and Lennard–Jones interactions, respectively, following MOIL protocols. Solvation effects were modeled implicitly using Gibbs–Born solvation scheme [23] as done in MOIL. The temperature was maintained at the desired value using velocity scaling. The glycosyl torsion χ was harmonically constrained with the force constant of 30 kcal/mol to be A-DNA-like ($\chi = 201.1^\circ$) and B-DNA-like ($\chi = 258.1^\circ$) in all simulations starting from north, and south energy minima, respectively, to mimic conditions in a polynucleotide chain. The dihedral angle γ was harmonically constrained at a value of 50° corresponding the *gauche* (g^+) conformation predominantly observed in A- and B-forms of DNA. The ensemble of structures generated from the different MD runs

was used to compute multiple SDE trajectories, as described below.

2.4. SDE trajectories

In total, 50 trajectories were computed between the north and south energy minima. Structures in C2′-endo and C3′-endo conformations were randomly selected from the ensemble generated above such that none of the coordinates were repeated. The parm99.dat version of the AMBER force field was used [28] with the solvent effects modeled implicitly using surface generalized Born model [23]. The AMBER force field had to be converted into format suitable for MOIL [19]. Prior to generating SDE trajectories, the force field was tested by performing several 10 ns ordinary MD simulations starting from the deoxyadenosine C2′-endo conformation and ensuring compatible trajectories.

Given the coordinates of deoxyadenosine C2′-endo and C3′-endo conformations, minimum energy paths were calculated and used as initial guesses for the SDE trajectories. The minimum energy paths were generated using the self-penalty walk (SPW) functional [22] with 101 grid points. The SPW minimizes the energies in the structures along the path generated by simple linear interpolation of Cartesian coordinates and provides a reasonable initial guess path. The paths were optimized for 10 000 steps. At the end of these minimum energy path calculations, the RMS distance between sequential structures was of the order of 0.1–0.2 Å.

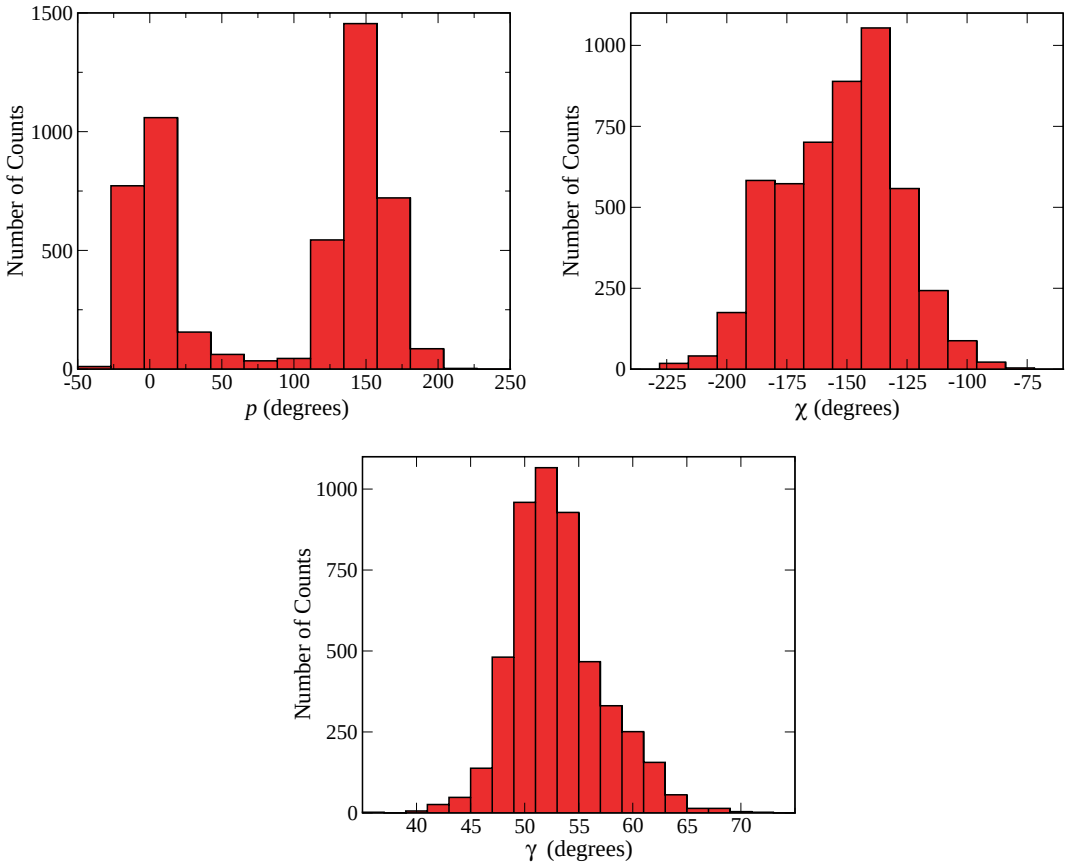

Fig. 2. Histograms of the deoxyadenosine sugar pucker pseudorotation phase angles p, glycosyl torsion χ, and backbone torsion γ from 50 SDE trajectories. The histograms were computed with a bin width of 23°, 12°, and 2°, respectively.

SPW calculations were further refined by the SDE formalism. The total energy of the system, E, was estimated from the standard initial-value molecular dynamics simulations that were equilibrated at room temperature. Both C3′-endo and C2′-endo conformations of deoxyadenosine were used to estimate the energy E. The target function T_G (or the path) was optimized by using five cycles of 2000 simulated annealing steps. The typical value of the gradient of the target function, T_G, normalized to the number of degrees of freedom, was 3.5 amu kcal/mol/Å. The simulated annealing temperatures varied linearly from 300 to 0.1 K during each cycle. The trajectories used in the analyses are described in the next section.

3. Results

The trajectories were analyzed for the torsional degrees of freedom χ, γ, and p which effectively characterize the overall conformation of deoxyadenosine. The histograms in Fig. 2 depict the probability distributions of χ, γ, and p collected over 50 trajectories. Clearly, the probability distributions for the glycosyl angle χ and backbone torsion γ are unimodal while that for the pseudorotation phase angle p is bimodal. Therefore, we express the potential of mean force $(W(p))$ as a function of p as follows:

$$W(p) = -k_B T \ln P(p), \tag{7}$$

where k_B is the Boltzmann constant, T is the temperature, and $P(p)$ is the probability distribution of phase angle of pseudorotation. The free energy plot $-k_B T \ln P(p)$ in units of kcal/mol is shown in Fig. 3. (The choice of p as the reaction coordinate is also supported by previous quantum mechanical studies [29–31], which suggested that there is no energy barrier separating low and high *anti* χ values.) The value of γ is well within the range from 0° to 120° with a mean value around 53° corresponding to g^+ conformation found predominantly in experimentally observed A- and B-DNA structures. We note that no assumption of equilibrium conditions nor of reaction coordinate was made in the path calculations.

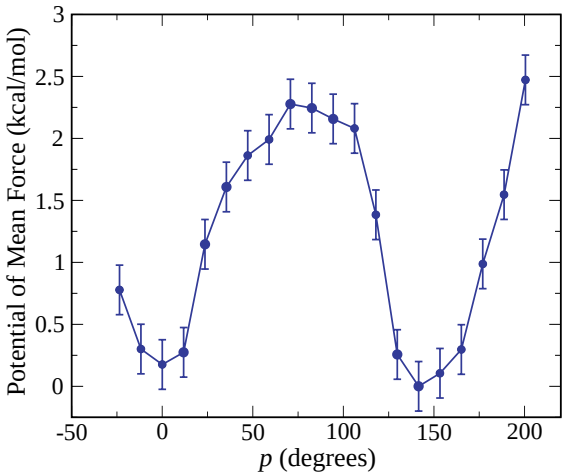

Fig. 3. A 'free energy' plot $-k_B T \ln P[p]$ as a function of the pseudorotation angle, p. $P(p)$ is the probability distribution of sugar pucker phase angle averaged over 50 trajectories connecting the C2′- and C3′-endo sugar conformations. The sugar pucker pseudorotation values and amplitudes were calculated based on Rao et al. [26] convention; see Eqs. (6) and (8) in text.

As Fig. 3 suggests, the transition between deoxyadenosine C2′-endo and C3′-endo conformations occurs through the east pseudorotation barrier with the highest energy barrier corresponding to the O4′-endo conformation (p in the range from 72° to 108°). The free energy difference (ΔG) corresponding to the transition from state C2′-endo to state O4′-endo is calculated as follows:

$$\Delta G = -k_B T \left[\ln \int_{\substack{p=62^\circ \\ (\mathrm{O4'\text{-}endo})}}^{p=108^\circ} P(p)\,\mathrm{d}p - \ln \int_{\substack{p=134^\circ \\ (\mathrm{C2'\text{-}endo})}}^{p=190^\circ} P(p)\,\mathrm{d}p \right]. \tag{8}$$

The highest observed energy barrier for the transition is 2.2 ± 0.2 kcal/mol above the global minimum. Our estimate of energy barrier falls well within the range calculated by other theoretical studies, given each method's approximations [9,10,14,17,20].

The deoxyadenosine south conformation is more stable than the north by a free energy difference of 0.34 ± 0.2 kcal/mol. The conformational free energy difference between C2′-endo and C3′-

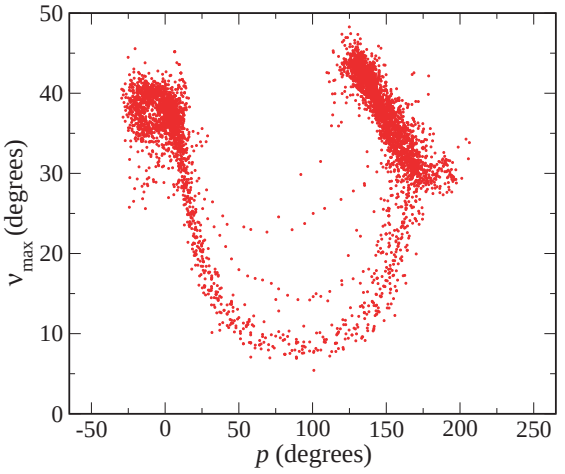

Fig. 4. Scatter plot of the sugar puckering amplitude (ν_{max}) as a function of the pseudorotation phase angle (p) for all structures observed in 50 trajectories connecting the deoxyadenosine C2′-endo and C3′-endo conformations. Note the decrease in puckering amplitude for $72° \leqslant p \leqslant 108°$.

endo conformations was computed using Eq. (8) except that the integration limits $-20° \leqslant p \leqslant 34°$. This estimate of energy difference is consistent with experimental and theoretical measurements [10,28,32].

The puckering amplitude ν_{max} decreases while passing over the east energy barrier (p in range from 72° to 108°) (Fig. 4). The average value of the amplitude, $\langle \nu_{max} \rangle$, in the O4′-endo region is 12°, suggesting that the puckering transition occurs through a high-energy planar intermediates. There is significant flattening of the ring around the barrier region. This result is in concordance with the results of Foloppe and MacKerell [15] who observed an amplitude of 18.1° in the O4′-endo state. The strain associated with the flattening of the furanose ring is believed to be the major contributor to the east energy barrier. As is well known, the west barrier ($p = 270°$) is highly unfavorable due to steric interactions between C1′ and C4′ substituents of the sugar ring.

4. Discussion

The conformational transition pathway of a deoxyadenosine nucleoside was investigated using the stochastic difference equation algorithm applied for first time to a nucleic acid system. The MOIL software was used to perform all the calculations using the AMBER version parm99 force field for nucleic acids, which we carefully incorporated and tested. The conformational free energy difference and free energy barrier between the C2′-endo and C3′-endo conformations of deoxyadenosine were determined from histogram analyses of 50 trajectories connecting the two states using SDE. As expected, the transition between the two predominant conformations was found to occur via the east energy barrier (O4′-endo conformation) with a decrease in the amplitude of furanose ring going over the east energy barrier. Our results are in good agreement with other theoretical studies as well as experiments that suggest a relatively low barrier that implies frequent interconversion.

Clearly, the behavior of the free nucleoside will be different from that in DNA, but we expect qualitative features of the free energy energy surface to be maintained. The SDE method we have used is based on a different physical approach and different approximations than used in prior studies of nucleic acid systems. Our benchmark computation shows that SDE has potential for large protein/DNA systems. Of course, the challenge of convergence of the free energy for a large system (due to large system size and large barriers) will have to be overcome. The present calculations are fast (e.g., generation of a single SDE trajectory takes 1 h of CPU time, and umbrella sampling to compute the free energy from a single optimal path takes about 2 h of CPU time, on an SGI Origin2000 300 MHz R120000 processor), but several months of computing time will be required for a macromolecular system of order of 50 000 atoms.

Acknowledgements

We are grateful to Prof. Ron Elber, Dr. Alfredo Cárdenas, and Ileana Stoica for making us available the latest code of MOIL and for technical assistance with its implementation. We thank the Elber lab for hosting K. Arora at Cornell and allowing him to gain experience with the SDE code. We thank Dr. Ravi Radhakrishnan for many

useful discussions regarding the free energy calculations. We thank the reviewer for pointing out recent accomplishments using QM/MM methodologies. This work was supported by NIH Grant R01 GM55164, NSF Grant ASC-9318159, and ACS-PRF 39115-AC4 Grant to T.S.

References

[1] T. Schlick, D. Beard, J. Huang, D. Strahs, X. Qian, IEEE Comput. Sci. Eng. 2 (2000) 38.
[2] T. Schlick, Molecular Modeling and Simulation: An Interdisciplinary Guide, Springer, New York, 2002.
[3] J. Florián, M.F. Goodman, A. Warshel, J. Am. Chem. Soc. 125 (2003) 8163.
[4] P. Ferrara, J. Apostolakis, A. Calfisch, Proteins 39 (2000) 252.
[5] B. Isralewitz, M. Gao, K. Schulten, Curr. Opin. Struct. Biol. 11 (2001) 224.
[6] R. Elber, A. Cardenas, A. Ghosh, H. Stern, Adv. Chem. Phys. 126 (2003) 93.
[7] A. Cardenas, R. Elber, Proteins 51 (2003) 245.
[8] S. Lifson, A. Warshel, J. Chem. Phys. 49 (1968) 5116.
[9] M. Levitt, A. Warshel, J. Am. Chem. Soc. 100 (1978) 2607.
[10] S.C. Harvey, M. Prabhakaran, J. Am. Chem. Soc. 108 (1986) 6218.
[11] H. Gabb, S.C. Harvey, J. Am. Chem. Soc. 115 (1993) 4218.
[12] W.K. Olson, P.J. Flory, Biopolymers 11 (1972) 25.
[13] W.K. Olson, J.L. Sussman, J. Am. Chem. Soc. 104 (1982) 270.
[14] W.K. Olson, J. Am. Chem. Soc. 104 (1982) 278.
[15] N. Foloppe, J.A.D. MacKerell, J. Phys. Chem. B 102 (1998) 6669.
[16] T. Schlick, C. Peskin, S. Bryode, M. Overton, J. Comput. Chem. 8 (1987) 1199.
[17] L. Nilsson, M. Karplus, J. Comput. Chem. 7 (1986) 591.
[18] L. Yang, W.A. Beard, S.H. Wilson, S. Broyde, T. Schlick, J. Mol. Biol. 317 (2002) 651.
[19] R. Czerminski, R. Elber, A. Roiterberg, C. Simmerling, R. Goldstein, H. Li, G. Verkhivker, C. Kesar, J. Zhang, A. Ulitsky, Comput. Phys. Commun. 91 (1995) 159.
[20] W.D. Cornell, P. Cieplak, C.I. Bayly, I.R. Gould, J.K.M. Merz, D.M. Feruguson, D.C. Spellmeyer, T. Fox, J.W. Caldwell, P.A. Kollman, J. Am. Chem. Soc. 117 (1995) 5179.
[21] R. Elber, A. Ghosh, A. Cardenas, Acc. Chem. Res. 35 (2002) 396.
[22] R. Czerminski, R. Elber, Int. J. Quantum Chem. 24 (1990) 167.
[23] G.D. Hawkins, C.J. Cramer, D.G. Truhlar, Chem. Phys. Lett. 246 (1995) 122.
[24] V. Tsui, D.A. Case, Biopolymers 56 (2000) 275.
[25] W.C. Still, A. Tempczyk, R.C. Hawley, T. Hendrickson, J. Am. Chem. Soc. 112 (1990) 6127.
[26] S. Rao, E. Westhof, M. Sundralingam, Acta Crystallogr. A 37 (1981) 421.
[27] C. Altona, M. Sundralingam, J. Am. Chem. Soc. 94 (1972) 8205.
[28] J. Wang, P. Cieplak, P.A. Kollman, J. Comput. Chem. 21 (2000) 1049.
[29] T.E. Cheatham, P. Cieplak, P.A. Kollman, J. Biomol. Struct. Dyn. 16 (1999) 845.
[30] N. Foloppe, J.A.D. MacKerell, Biophys. J. 76 (1999) 3206.
[31] N. Foloppe, B. Hartmann, L. Nilsson, J.A.D. MacKerell, Biophys. J. 82 (2002) 1554.
[32] D.R. Davis, Prog. Nucl. Magn. Reson. Spectrosc. 12 (1978) 135.